



# Human Gestational *N*-Methyl-D-Aspartate Receptor Autoantibodies Impair Neonatal Murine Brain Function

Betty Jurek, PhD,<sup>1,2\*</sup> Mariya Chayka, MD,<sup>1,2\*</sup> Jakob Kreye, MD,<sup>1,2</sup> Katharina Lang, MD,<sup>1,2</sup> Larissa Kraus, MSc,<sup>1,3,4</sup> Pawel Fidzinski, MD,<sup>1,3</sup> Hans-Christian Kornau, PhD,<sup>2,5</sup> Le-Minh Dao, PhD,<sup>1,2</sup> Nina K. Wenke, PhD,<sup>2</sup> Melissa Long, BSc,<sup>6</sup> Marion Rivalan, PhD,<sup>6</sup> York Winter, PhD,<sup>6</sup> Jonas Leubner, MD,<sup>1</sup> Julia Herken, <sup>1</sup> Simone Mayer, PhD,<sup>7</sup> Susanne Mueller, PhD,<sup>1,8,9</sup> Philipp Boehm-Sturm, PhD,<sup>1,8,9</sup> Ulrich Dirnagl, MD ,<sup>1,2,9</sup> Dietmar Schmitz, MD,<sup>2,5,10</sup> Michael Kölch, MD,<sup>11</sup> and Harald Prüss, MD ,<sup>1,2,12</sup>

**Objective:** Maternal autoantibodies are a risk factor for impaired brain development in offspring. Antibodies (ABs) against the NR1 (GluN1) subunit of the *N*-methyl-D-aspartate receptor (NMDAR) are among the most frequently diagnosed anti-neuronal surface ABs, yet little is known about effects on fetal development during pregnancy.

**Methods:** We established a murine model of in utero exposure to human recombinant NR1 and isotype-matched non-reactive control ABs. Pregnant C57BL/6J mice were intraperitoneally injected on embryonic days 13 and 17 each with 240 µg of human monoclonal ABs. Offspring were investigated for acute and chronic effects on NMDAR function, brain development, and behavior.

**Results:** Transferred NR1 ABs enriched in the fetus and bound to synaptic structures in the fetal brain. Density of NMDAR was considerably reduced (up to −49.2%) and electrophysiological properties were altered, reflected by decreased amplitudes of spontaneous excitatory postsynaptic currents in young neonates (−34.4%). NR1 AB-treated animals displayed increased early postnatal mortality (+27.2%), impaired neurodevelopmental reflexes, altered blood pH, and reduced bodyweight. During adolescence and adulthood, animals showed hyperactivity (+27.8% median activity over 14 days), lower anxiety, and impaired sensorimotor gating. NR1 ABs caused long-lasting neuropathological effects also in aged mice (10 months), such as reduced volumes of cerebellum, midbrain, and brainstem.

**Interpretation:** The data collectively support a model in which asymptomatic mothers can harbor low-level pathogenic human NR1 ABs that are diaplacentally transferred, causing neurotoxic effects on neonatal development. Thus, AB-mediated network changes may represent a potentially treatable neurodevelopmental congenital brain disorder contributing to lifelong neuropsychiatric morbidity in affected children.

ANN NEUROL 2019;86:656–670

View this article online at [wileyonlinelibrary.com](http://wileyonlinelibrary.com). DOI: 10.1002/ana.25552

Received Oct 14, 2018, and in revised form Jul 12, 2019. Accepted for publication Jul 15, 2019.

Address correspondence to Dr Prüss, German Center for Neurodegenerative Diseases (DZNE) Berlin, c/o Charité–Universitätsmedizin Berlin, CharitéCrossOver, Room 4-119, Charitéplatz 1, 10117 Berlin, Germany. E-mail: [harald.pruess@charite.de](mailto:harald.pruess@charite.de)

Current address for Dr Mayer: Hertie Institute for Clinical Brain Research, University of Tübingen, 72076 Tübingen, Germany.

\*B.J. and M.C. contributed equally to this work.

From the <sup>1</sup>Department of Neurology and Experimental Neurology, Charité–Universitätsmedizin Berlin, Berlin, Germany; <sup>2</sup>German Center for Neurodegenerative Diseases (DZNE) Berlin, Berlin, Germany; <sup>3</sup>Clinical and Experimental Epileptology, Charité–Universitätsmedizin Berlin, Berlin, Germany; <sup>4</sup>Berlin Institute of Health, Berlin, Germany; <sup>5</sup>Neuroscience Research Center, Charité–Universitätsmedizin Berlin, Berlin, Germany; <sup>6</sup>Neurocure Cluster of Excellence, Animal Outcome Core Facility, Charité–Universitätsmedizin Berlin, Berlin, Germany; <sup>7</sup>Eli and Edythe Broad Center of Regeneration Medicine and Stem Cell Research and Department of Neurology, University of California, San Francisco, San Francisco, CA; <sup>8</sup>Neurocure Cluster of Excellence, Core Facility 7T Experimental MRIs, Charité–Universitätsmedizin Berlin, Berlin, Germany; <sup>9</sup>Center for Stroke Research, Charité–Universitätsmedizin Berlin, Berlin, Germany; <sup>10</sup>Einstein Center for Neurosciences, Berlin, Germany; <sup>11</sup>Department for Child and Adolescent Psychiatry, Neurology, Psychosomatics, and Psychotherapy, Universitätsmedizin Rostock, Rostock, Germany; and <sup>12</sup>Department of Neurology, Center for Autoimmune Encephalitis and Paraneoplastic Neurological Syndromes, Charité–Universitätsmedizin Berlin, Berlin, Germany

Proper fetal development in mammals requires complex mechanisms regulated from both fetus and mother. One maternal immune mechanism to protect the fetus is passive immunity, where maternal immunoglobulin G (IgG) is transferred via neonatal Fc receptors (FcRn).<sup>1</sup> Transfer of maternal antibodies (ABs) in humans starts from gestational week 13 in the second trimester,<sup>2</sup> when the fetal blood–brain barrier (BBB) is still permeable,<sup>3</sup> creating a critical window for potentially harmful anti-neuronal ABs to compromise fetal brain development. Maternal immune activation including such ABs may therefore influence the etiology of neurodevelopmental disorders, including autism spectrum disorders (ASD), learning disabilities, and schizophrenia.<sup>4,5</sup>

Murine models of gestational transfer of maternal ABs have already revealed deleterious effects of some anti-neuronal ABs, for example, anti-NR2B (GluN2B),<sup>6</sup> anti-fetal brain ABs from mothers of children with ASD,<sup>7,8</sup> and anti-Caspr2 ABs.<sup>9,10</sup> So far, little is known about maternal ABs against the NR1 (GluN1) subunit of the *N*-methyl-D-aspartate receptor (NMDAR), although it is among the most frequent anti-neuronal ABs in clinically asymptomatic individuals, with an IgG seroprevalence of 1%.<sup>11,12</sup> This creates a considerable subgroup of pregnancies in which NR1 ABs can be diaplacentally transferred. A pathogenic role for impairment of fetal brain development by such ABs seems possible for several reasons. First, monoclonal human NR1 ABs cloned from anti-NMDAR encephalitis patients were directly pathogenic by disrupting synaptic NMDAR currents.<sup>13</sup> Second, in vitro and in vivo studies in adult animals demonstrated human NR1 AB-mediated internalization of NMDARs, resulting in NMDAR hypofunction.<sup>14–16</sup> Third, during fetal brain development, NMDARs are crucial for proper axonal<sup>17</sup> and dendritic growth,<sup>18</sup> neuronal survival,<sup>19</sup> and glutamatergic synaptic transmission at early stages.<sup>20</sup> Fourth, animal models of NMDAR hypofunction during neurodevelopment, induced by either transient NMDAR blockage<sup>21</sup> or NR1 mutations,<sup>22</sup> were characterized by major developmental deficits, for example, growth retardation and impaired cognitive functions.

We therefore hypothesized that maternally transferred NR1 ABs can cause fetal NMDAR hypofunction, leading to impaired brain development and sustained deficits persisting into childhood and possibly adulthood. If verified, this could have far-reaching clinical implications, including therapeutic options to prevent developmental brain abnormalities and lifelong psychiatric morbidity in affected children. Hence, we established a mouse model of gestational transfer of human monoclonal NR1 ABs and determined effects on NMDAR function, brain development, and behavior in the offspring.

## Materials and Methods

### Animal Experiments

Animal experiments were carried out in accordance with the ARRIVE guidelines, the EU directive (2010/63/EU) for animal experiments, and were approved by the local ethics committee for Animal Welfare (LaGeSO, Berlin, G0175/15).

At gestational days E13 and E17, 8- to 10-week-old pregnant C57BL/6J mice were either not treated ( $n = 6$ ) or injected intraperitoneally with 240 $\mu$ g human monoclonal IgG1 ABs each (nonreactive control clone: #mGo53 [ $n = 40$ ; CTL], high-affinity NR1-reactive [amino-terminal domain] IgG1 clone: #003-102 [ $n = 47$ ; NR1])<sup>13,23,24</sup> in sterile phosphate-buffered saline (PBS). Further controls included identical amounts of monoclonal IgG1 ABs against glial fibrillary acidic protein (GFAP; clone: #011-116<sup>13</sup> [ $n = 15$ ]) and human immunoglobulins (intravenous immunoglobulin [IVIG]; Grifols, Barcelona, Spain [ $n = 15$ ]). AB amounts were 10- to >100-fold lower than in comparable passive immunization studies<sup>25,26</sup> and resulted in maternal serum NR1 AB levels of 1:100 to 1:320 in routine cell-based assays. Animals were sacrificed as indicated in Figure 1. Offspring were housed in treatment-mixed groups of 2 to 5 mice of both sexes.

### Production of Human Monoclonal ABs

Recombinant human monoclonal NR1-reactive IgG1 ABs (clones #003-102 and #007-168) were generated from 2 female patients with acute NMDAR encephalitis and produced together with a nonreactive human monoclonal isotype-matched ABs (#mGo53) and an anti-GFAP ABs (#011-116) as described previously.<sup>13,27</sup> All ABs were IgG1; these cross the human placenta and murine yolk sac with highest efficiency of all IgG subclasses.<sup>28,29</sup>

### Fetal AB Distribution

Embryos were harvested at E19, and whole embryo sections were methanol-fixed and stained with rat anti-CD31 (1:150; BD Biosciences, Franklin Lakes, NJ; #55370), rabbit anti-VGLUT1 (1:500; Synaptic Systems, Göttingen, Germany; #135303), and rabbit-anti-NR1 (1:250; Merck, Darmstadt, Germany; #AB9864). Secondary ABs included goat anti-human IgG-488 (1:1,000; Dianova, Hamburg, Germany; #109-095-003), goat anti-rabbit-568, and goat anti-rat-568 (1:1,000; Life Technologies, Carlsbad, CA; #A11036, #A11077).

### Serum AB Kinetics

Trunk blood from postnatal day (P) 0, P7, P10, and P14 pups and respective dams was taken by decapitation, and human AB levels were determined using a commercial antihuman IgG enzyme-linked immunosorbent assay (ELISA; Mabtech, Nacka Strand, Sweden).

### IgG Extraction from Mouse Brain

Brain-bound IgG in immunized pups was extracted from whole unperfused brains at P0 and P7 by an acid-based method adapted from a previous protocol.<sup>15</sup> Brains from P0/P7 pups (~100/200mg) were homogenized in 6/10ml PBS with

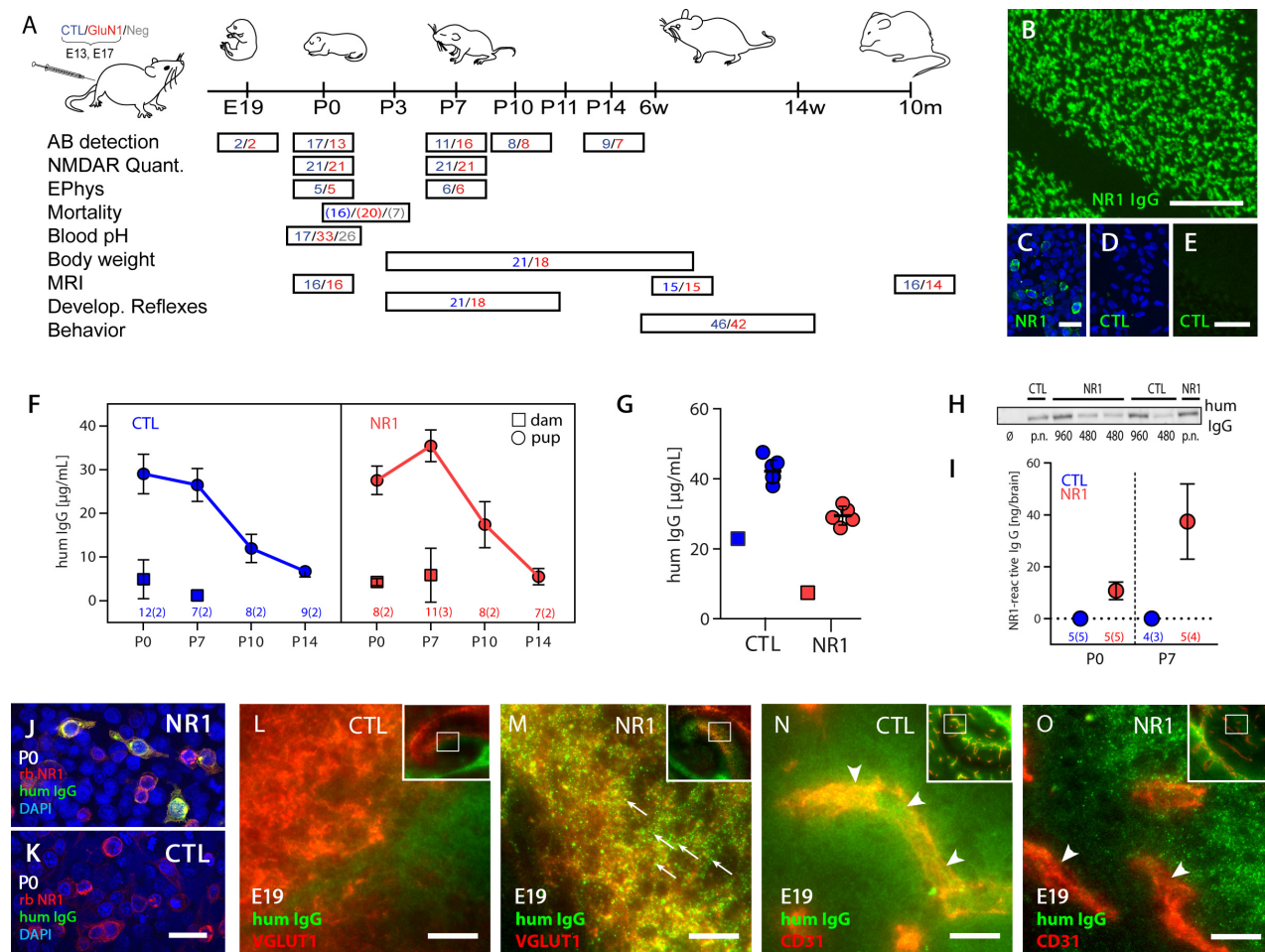


**FIGURE 1:** Experimental design and characterization of transfer of antibodies (ABs) in a gestational mouse model of maternal NR1 ABs. (A) Experimental design for characterization of AB transfer and neonatal development at different time points (n = pups; litters in parentheses) of control (CTL)/NR1/untreated dams. Blue = control, red = NR1, gray = untreated. (B, C) Human recombinant monoclonal NR1 ABs used for this study showed the typical staining on murine brain sections, for example, granular cells in cerebellum (B), and on NR1-transfected HEK cells (C). (D, E) The nonreactive human control ABs used throughout this study did not bind NR1-expressing HEK cells (D) or brain tissue (E). (F) Injected human ABs were transferred into the neonatal circulation with the highest concentrations at postnatal day (P) 0 for CTL and at P7 for NR1 AB-treated offspring, with declining level afterward. (G) AB injections into dams starting only postnatally (P0 and P3) resulted in high levels of neonatal ABs in both groups (P7), confirming that IgG ABs were also sufficiently transferred via breast milk. (H) Western blot (cropped) of neonatal brains detected human IgG in both CTL and NR1 AB-treated animals (960µg per dam; 480µg; ∅ = untreated; p.n. = postnatal injection [480µg]). (I) Enzyme-linked immunosorbent assay quantification of NR1-specific ABs in brain IgG extracts revealed increasing levels of brain-bound IgG from P0 (mean = 10.7ng) to P7 (mean = 37.4ng) in the NR1 group. (J, K) Brain IgG extracts from NR1 AB-immunized neonates (P0) retained their binding capability to NR1 (J), whereas extracted IgG from the CTL group did not show any binding (K). (L, N) CTL ABs distributed diffusely in the fetal brain (L), mainly around blood vessels (N, arrowheads). (M, O) In contrast, NR1 ABs colocalized with punctate presynaptic VGLUT1 clusters (M, some clusters depicted with arrows), mainly outside vessels in the brain parenchyma (O). Inserts show the area of the micrograph in the hippocampus (L–O). Scale bars: B, E, 100µm, C, D, J, K, 20µm; L–O, 100µm. E = embryonic day; EPhys = electrophysiology; hum = human; MRI = magnetic resonance imaging; NMDAR = N-methyl-D-aspartate receptor; rb = rabbit.

proteinase inhibitors (PBS-PI; Roche, Basel, Switzerland; cOmplete ethylenediaminetetraacetic acid [EDTA]-free tablets). Six milliliters each were centrifuged, and the pellet was washed 3 times with 1ml PBS-PI to eliminate unbound IgG located in blood vessels. For extraction of bound IgG, the pellet was dissolved for 5 minutes in 258µl 0.1M Na-citrate buffer (pH 2.7) and centrifuged, and the supernatant was neutralized with 52µl 1.5M Tris (pH 8.8). Supernatant of the last wash (with 0.3ml) was analyzed as pre-extraction fraction to exclude residual free human IgG in the extract.

### ELISA Quantification of Human NR1 ABs in Brain Extracts

Concentration of recombinant human NR1 AB #003-102 in brain extracts was determined in 96-well plates coated overnight at 4°C with donkey anti-rabbit IgG (20µg/ml, Dianova, #711-005-152). After blocking with 2% bovine serum albumin (BSA) in PBS/0.05% Tween-20 (PBS/T) at room temperature (RT), cell culture supernatants of HEK293 cells that expressed the amino-terminal domain (amino acids 1–400) of human NR1 fused to rabbit Fc were applied. Mouse brain extracts were

diluted 1:25/1:100 in 0.4% BSA-PBS/T and added in duplicates. Plates were washed with PBS/T and incubated with horseradish peroxidase (HRP)-conjugated donkey anti-human IgG (1:5,000, Dianova, #709-035-149). After washing, HRP activity was measured using 1-Step Ultra TMB-ELISA substrate (Thermo Fisher Scientific, Waltham, MA). The concentrations of #003-102 in the extracts were deduced from a calibration curve generated with purified #003-102.

### NR1-Specific Cell-Based Assay

NR1-transfected HEK cells were grown on coverslips, methanol-fixed, blocked for 30 minutes, incubated overnight with murine sera or IgG extracted from neonatal brains, and visualized as described.<sup>13</sup>

### Quantification of NR1 Protein, GluR1, and Human IgG with Western Blots

Synaptosomal fractions were prepared from P0 pups with SYNPER (Life Technologies, #87793). For membrane and total fractions, brains from P0 and P7 mice were homogenized in 10 volumes of homogenization buffer (0.32M sucrose, 10mM hydroxyethylpiperazine ethane sulfonic acid [HEPES] pH 7.4, 2mM EDTA) and centrifuged at  $1,000 \times g$  for 10 minutes to remove nuclear fraction. An aliquot of supernatant was kept as total fraction. The remainder was centrifuged at  $10,000 \times g$  for 15 minutes, and supernatant was centrifuged at  $100,000 \times g$  for 60 minutes. Pellets from P0 and P7 pups were resuspended in 100 and 300 $\mu$ l sample buffer, respectively. CTL and NR1 AB-treated samples were loaded on 8% acrylamide gels, transferred via TurboBlot (Bio-Rad Laboratories, Hercules, CA) onto nitrocellulose, blocked, stained with rabbit-anti-NR1 (1:1,000, Merck, #AB9864) or rabbit anti-GluR1 (1:8,000; Millipore, Billerica, MA; #AB1504), and incubated with goat anti-rabbit IgG-HRP (1:6,000; Vector Laboratories, Burlingame, CA; #PI-1000). Membranes were developed with Western Lightning (PerkinElmer, Waltham, MA). Consecutive incubation was carried out with primary ABs for reference proteins (synaptosomal and total cell fraction: mouse anti-mortalin, 1:5,000, NeuroMab [Davis, CA], #75-217; membrane fraction: rabbit anti- $\beta$ -actin, 1:3,000, Sigma-Aldrich [St Louis, MO], #A5060) and respective secondary ABs.

### Quantification of NR1 Protein Expression with Immunohistochemistry

NMDAR clusters were detected with human monoclonal AB clone #007-168. To exclude that this monoclonal "detection AB" competes with the "treatment AB" (#003-102) for the same epitope, 1mg of each AB was labeled with 8.4 $\mu$ l CruzFluor 488 succinimidylester (10mg/ml; Santa Cruz Biotechnology, Santa Cruz, CA; #sc-362617). Murine brain sections were incubated with a fixed concentration of labeled AB plus increasing concentrations of either the identical unlabeled AB, the other AB (competition assay), or a control AB (Homer-1, Synaptic Systems, #160004). For NR1 cluster analysis, brain sections were incubated for 48 hours at 4°C with Homer-1 (1:200) and #007-168-Biotin (biotinylation kit, Thermo Fisher Scientific,

#QE217779, 15 $\mu$ g/ml), followed by goat anti-guinea pig-568 (Invitrogen, Carlsbad, CA; #A-11075) and streptavidin-488 (Invitrogen, #A-32360). Two pictures from the CA3 region were taken from 3 individuals of  $\geq 3$  litters. Homer-1-positive synaptic sites were marked manually, and fluorescence intensities for human NR1 AB #007-168 were calculated automatically for each marked site and corrected for background fluorescence. Overlapping puncta of Homer-1 and human NR1 were counted and displayed as ratio of colocalized to synaptic puncta.

### Electrophysiological Recordings

Horizontal hippocampal vibratome slices (350 $\mu$ m) from P0 or P7 pups of CTL and NR1 AB-immunized dams were transferred to a submerged holding chamber and stored in artificial cerebrospinal fluid (in mM: 129 NaCl, 1.25 NaH<sub>2</sub>PO<sub>4</sub>, 1.6 CaCl<sub>2</sub>, 3.0 KCl, 1.8 MgSO<sub>4</sub>, 21 NaHCO<sub>3</sub>, 10 glucose) at 32 to 35°C for 30 minutes, followed by RT until recording. Whole-cell patch clamp recordings on CA1 pyramidal neurons were performed with borosilicate pipettes (1.5mm outer diameter) filled with internal solution containing (in mM) 125 CsCl, 2 Mg<sub>2</sub>Cl, 10 HEPES, 2 ethyleneglycoltetraacetic acid, 2 Na<sub>2</sub>ATP, 0.3 NaGTP. Access resistance did not exceed 20M $\Omega$  and varied less than 20%. Signals were low-pass filtered at 2kHz and sampled at 10kHz. Spontaneous excitatory postsynaptic currents (sEPSCs) were recorded at -70mV for at least 4 minutes. To avoid depolarizing  $\gamma$ -aminobutyric acid (GABA) currents, GABAA-R antagonist SR-95531 was applied (1 $\mu$ M; Tocris Bioscience, Bristol, UK).

### Determination of Blood pH

P0 pups from CTL and NR1 AB-treated animals were decapitated, and trunk blood was mixed with 2 volumes of heparinized NaCl to reach the minimal volume required for analysis with an ABL-800 system (Radiometer, Brønshøj, Denmark).

### Measurements of Activity

Transponders were implanted into offspring at 12 to 14 weeks. Activity was tracked for 14 days with a Social Activity Monitoring system (PhenoSys, Berlin, Germany) based on an ID-Grid sensor plate recording individual spatiotemporal information.

### Magnetic Resonance Imaging-Based Determination of Brain Volume

Magnetic resonance imaging (MRI) was performed on P0 pups and adult mice using a 7T small animal scanner (7T BioSpec +1H-Cryoprobe; Bruker, Karlsruhe, Germany). Animals were euthanized using isoflurane. Volumes of P0 animals were assessed using a high-resolution morphological T2-weighted TurboRARE sequence (repetition time/echo time = 4,000/34.5 milliseconds, 10 averages, rapid acquisition with relaxation enhancement [RARE] factor = 8, 36 coronal slices per 0.25mm, field of view = 12.8  $\times$  12.8mm<sup>2</sup>, matrix = 170  $\times$  170, in-plane resolution = 75  $\times$  75 $\mu$ m<sup>2</sup>, scan time = 14 minutes). Volumetry was performed using Analyze 10.0 software (AnalyzeDirect, Overland Park, KS). For adult mice (repetition time/echo time = 4,250/33 milliseconds, 2 averages, RARE factor = 8,

40 coronal slices per 0.40mm, field of view =  $19.2 \times 19.2$  mm<sup>2</sup>, matrix =  $192 \times 192$ , in-plane resolution =  $100 \times 100$  μm<sup>2</sup>, scan time = 3 minutes 24 seconds, volumetry was performed automatically using the MATLAB (MathWorks, Natick, MA) toolbox ANTX to nonlinearly register magnetic resonance images to the Allen brain atlas.<sup>30</sup>

### Neurodevelopmental Scoring

Neonates were scored from days P3 to P56 based on established protocols.<sup>31</sup> The cutoff for surface righting reflex, cliff avoidance, and negative geotaxis reflex was 30 seconds.

### Behavioral Assessment

A modified SHIRPA test to identify general abnormalities<sup>32</sup> showed a normal phenotype in all offspring prior to behavioral assessment.

**Three-Chamber Test (Sociability).** After 10 minutes of habituation to a 3-chambered arena for 6-week-old mice, an empty cage and a cage containing an unfamiliar C57BL/6J mouse (same sex) were placed in opposite side chambers. The location of cages was systematically alternated between animals. The number of times mice entered the chambers and came close to the cages were recorded by the video tracking system Viewer-3 (Biobserve, Bonn, Germany).

**Barnes Maze.** Seven-week-old mice were tested for learning and memory in a Barnes maze. They were trained for 4 days on a white platform to find a hidden escape box under 1 of 20 holes. Orientation cues were placed around the platform on the wall. Behavior and distance traveled into the 4 quadrants were recorded with Viewer-3. Cutoff was 180 seconds during training (4 trials every day for 4 days) and 90 seconds during testing (days 5 + 12, memory recall during 90 seconds).

**Elevated Plus Maze.** Eight-week-old mice on a white polyvinyl chloride (50 × 50 × 53cm) elevated plus maze with 2 open arms and 2 closed arms explored for 5 minutes, then activity was tracked using Viewer-3.

**Prepulse Inhibition.** Each test session in 9-week-old mice consisted of 5 trial types according to established protocols<sup>33</sup>: white noise (N56dB), acoustic startle (P120dB, 40 milliseconds), and 3 prepulse acoustic startle trials (PP69dB, PP73dB, and PP81dB for 20 milliseconds, 100 milliseconds before acoustic startle of P120dB for 40 milliseconds). Each session started with 10 minutes of acclimation, then 5 acoustic startle trials (P120dB), followed by 10 blocks of the 5 prepulse trials (PP69dB–P120dB, PP73dB–P120dB, PP81dB–P120dB) in pseudorandom order and another 5 acoustic startle trials (P120dB). Inter-trial intervals ranged between 12 and 30 seconds.

**Home Cage Scan.** Natural behaviors in the home cage of freely moving mice were determined over 24 hours using HomeCageScan software (CleverSys, Reston, VA), including durations of grooming, twitching (indicator for repetitive behavior), consumption (eating and drinking), and sleeping.

**Nest Construction Test.** Nestlets (5 × 5cm squares of pressed white cotton) were placed in the cage on 2 consecutive days, and the nest was scored the next day for complexity according to established protocols.<sup>34</sup> The remaining intact nestlet material was weighed.

### Flow Cytometry–Based Quantification of NR1 Reactivity in Human Maternal Sera

Serum from 120 healthy mothers of children with psychiatric disorders (MCPD) and 105 serum samples from healthy control mothers of unaffected children (CTLM) were collected at the Vivantes Department for Child and Adolescent Psychiatry, Berlin-Friedrichshain, Germany. NR1 autoreactivity was quantified in a flow cytometry–based approach using live HEK cells overexpressing native human NR1 protein as described previously.<sup>23</sup>

### Methods to Prevent Bias

Pregnant dams were randomly assigned for injection. After weaning, mice of both treatment groups were mixed-housed. Within all experiments, animals or samples were used in an alternating manner. The investigator was blinded to group allocation and analysis for MRI, electrophysiology, and NR1-positive cluster quantification. For behavioral paradigms, sample size was determined by publicly available datasets, extracted numeric data by the use of PlotDigitizer (<http://plotdigitizer.sourceforge.net/>), and subsequent a priori power analysis using G\*Power (<http://www.gpower.hhu.de/>).

### Statistical Analysis

Statistical analyses were performed with Prism 7 (GraphPad Software, San Diego, CA) and R (<https://www.r-project.org/>). Data are presented as scatterplots with mean ± standard deviation or median with 95% confidence interval. Statistical analyses included *t* test, analysis of variance (ANOVA), and repeated measurement ANOVA following Holm–Sidak or Tukey multiple comparison test. Mann–Whitney and Kruskal–Wallis tests were used for non-parametric data, followed by Dunn multiple comparison test. Wilcoxon test was used to compare total activity of animals, 1-sided Fisher exact test for frequency distribution, and Kaplan–Meier log-rank test for survival with Bonferroni correction; *p* < 0.05 was considered statistically significant.

## Results

### Human NR1 ABs Were Diaplacentally Transferred and Bound to Synaptic Structures within the Neonatal Brain

Human monoclonal recombinant NR1 IgG1 ABs and isotype-matched nonreactive CTL ABs were injected at gestational days E13 and E17 (240μg each), and AB-mediated effects were investigated in the offspring at

different developmental stages (see Fig 1). Monoclonal human NR1 ABs used in this study showed the characteristic binding on murine brain sections, for example, to granular cells in the cerebellum and to NR1 protein in routine cell-based assays, whereas CTL ABs were non-reactive on NR1-transfected cells and brain sections. ELISA quantification in murine serum confirmed that human IgG were transferred into and enriched in neonates (up to P7 in NR1 AB-treated mice) with declining levels afterward. Injections starting postpartum proved transfer of human IgG also via breast milk. Western blot analyses detected comparable amounts of human total IgG in the brains of NR1 and CTL AB-treated animals. NR1-specific human IgG was found in neonatal whole brain extracts via ELISA only following prenatal NR1 AB injections with increasing concentrations between P0 and P7.

We next examined whether brain-accumulated NR1 ABs retained the capability of binding the NMDAR. Extracts of brain-bound IgG from NR1 AB-treated but not from CTL AB-treated animals were reactive to NR1-transfected HEK cells at days P0 (see Fig 1J, K) and P7 (not shown). The anatomical distribution was strikingly different between groups, as confirmed with immunohistochemical colabeling of fetal brain tissue (E19). Whereas CTL ABs were diffusely distributed in proximity to CD31-positive blood vessels, NR1 ABs overlapped with the presynaptic marker VGLUT1 in a characteristic punctate parenchyma pattern not confined to vasculature (see Fig 1).

### **Maternal NR1 ABs Reduced NMDAR Density and Changed Electrophysiological Properties in Early Postnatal Life**

Observed binding of human ABs to NR1 led to the question of whether transferred ABs reduce density of NMDAR in the neonatal brain. Western blots of purified synaptosomes showed a significantly reduced density in NR1 AB-treated neonates, indicating profound loss of synaptic NMDAR, which was absent at P7 (Fig 2). Similarly, brain membrane fractions and total-cell fractions contained significantly less NR1 protein than in CTL AB-treated animals at P0, but returned to normal levels at P7. As a control, NR1 AB-treated animals showed no reduction of  $\alpha$ -amino-3-hydroxy-5-methyl-4-isoxazolepropionic acid receptors (AMPA; GluR1) in total-cell fractions at P0. Corresponding histological quantification of NMDAR clusters colocalizing with synaptic Homer-1 revealed strong reduction (up to 49.2%) in synaptic NMDAR cluster densities in the early postnatal brain, which was less marked at P7. The human monoclonal NR1 AB used for detection (#007-168) did not compete with the

human treatment AB (#003-102) or the Homer-1 AB. Reduction of synaptic NMDAR was paralleled by electrophysiological changes in brain slices. NR1 AB-treated animals at day P0 showed significantly reduced amplitudes of sEPSCs, which normalized until P7. The frequency of sEPSCs was not altered.

### **Increased Mortality and Altered Physiological Parameters in NR1 AB-Exposed Offspring**

NR1 AB-treated neonates displayed significantly reduced survival rates within the first 3 postnatal days (66.7%) compared to CTL AB-treated (#mGo53, 93.9%; GFAP, 100%; IVIG, 100%) and untreated (95.2%) offspring (Fig 3). Survival rates markedly varied in the NR1 group, ranging from 0 to 100%, whereas they never fell below 60% in controls. As animals did not die later than P3, we investigated vegetative functions related to acid–base metabolism early after birth. Blood gas analysis showed a highly significantly elevated blood pH in NR1 AB-treated neonates. Surviving animals in the NR1 group gained less body weight during breastfeeding. The difference persisted after weaning during adolescence in both female and male mice and diminished in adulthood (8 weeks). Changes were not attributable to dysfunctional maternal behavior, as dams were asymptomatic, and showed normal maternal care (pup retrieval test<sup>35</sup>), breastfeeding, and nesting (data not shown), and the litter size was not different excluding prepartum death of embryos. Whole brain volumes and hippocampal volumes were not affected between both groups at birth using MRI. However, brain volumes were significantly reduced in the NR1 AB-treated offspring after 8 weeks and 10 months. The strongest reduction was detectable in cerebellum, midbrain, and brainstem (Table 1). Activity recordings revealed significantly higher baseline activity (+27.8% comparing median over 14 days) in the home cages of NR1 AB-treated animals during the dark (active) phase.

### **Maternal NR1 ABs Delayed Neurodevelopment in Neonates, Reduced Anxiety Behavior, and Impaired Prepulse Inhibition in Adult Offspring**

We next examined whether the development of early postnatal reflexes was impaired. Compared to controls, mice of the NR1 group had significantly reduced abilities for righting between P5 to P8 (Fig 4). Similarly, development of the cliff avoidance reflex was significantly impaired, and the negative geotaxis reflex was significantly delayed between P4 and P9 in NR1 AB-treated animals. During adolescence (6–7 weeks), animals of both groups had similar social preference in the 3-chamber test and equal abilities in spatial learning and memory in the Barnes maze test. NR1 animals at 9 weeks showed decreased prepulse

inhibition (PPI; -8.9%) at 69dB only, indicating subtle changes in sensorimotor gating function that persisted into adulthood. Likewise, NR1 AB-treated animals spent more time in and entered more often the open arms of the elevated plus maze, which was not related to faster locomotion, thus indicating lower anxiety. In the home cage, nests built by either group were similarly complex, and the naturally expressed behaviors (ie, climbing, drinking, sleeping) did not quantitatively differ between groups.

**Serum Anti-NR1 IgG Reactivity in Mothers of Children with Psychiatric Disorders**

To estimate whether NR1 autoreactivity can also be found in the serum of human mothers, we compared samples of 120 MCPD versus 105 CTLM. Children from MCPD had various psychiatric disorders ranging from hyperkinetic or emotional disorders to depressive episodes and pervasive developmental disorders; the pregnancies were 4 to 20 years before serum sampling (Table 2). Using our

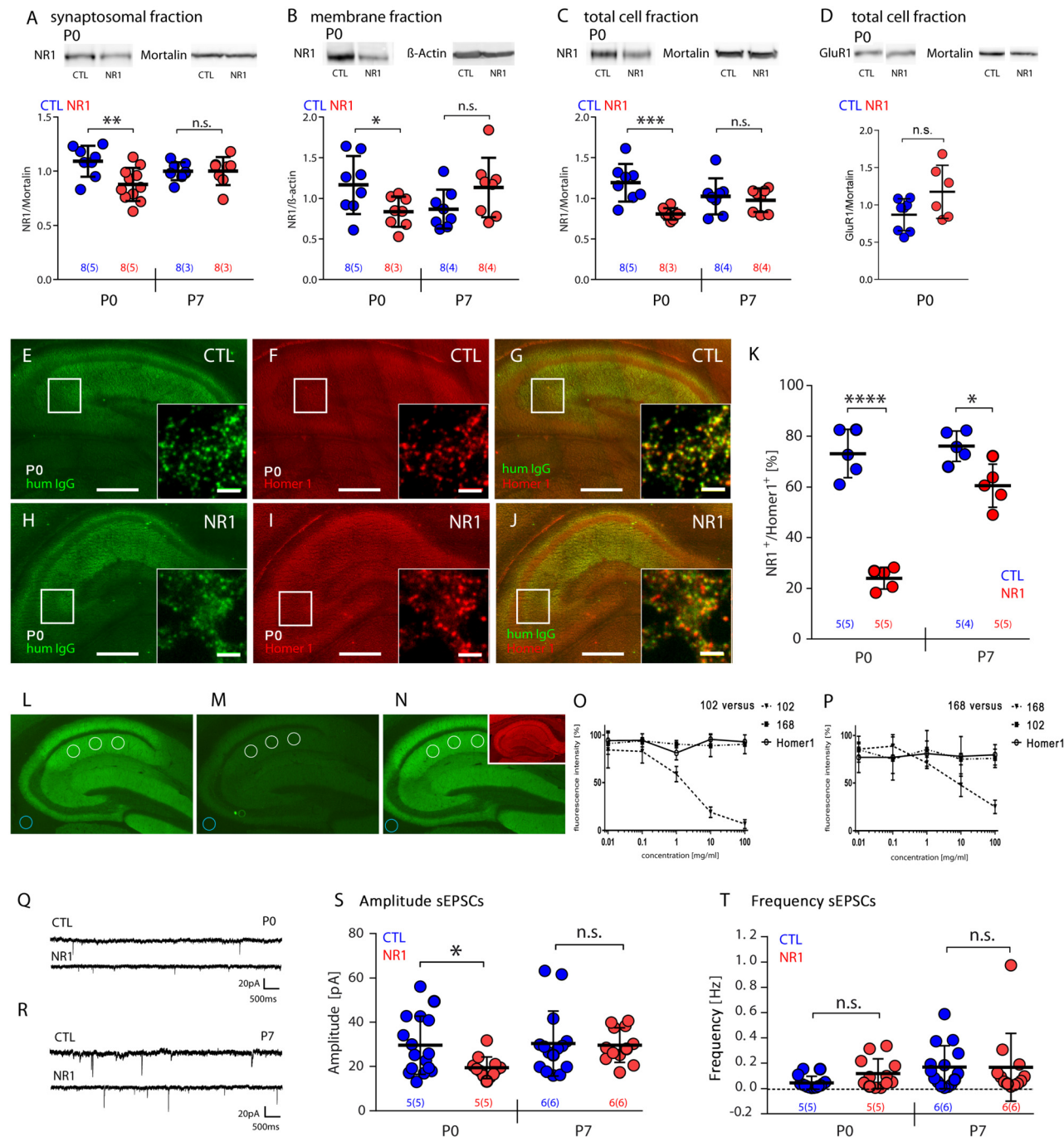


FIGURE 2: Legend on next page.

flow cytometry–based approach to objectively measure the continuous spectrum of NR1 IgG autoreactivity, titers were slightly higher in MCPD samples compared to CTLM ( $p = 0.038$ ; Fig 5). Dose-titration curves with human monoclonal NR1 ABs and isotype-matched non-reactive CTL ABs revealed high sensitivity with flow cytometry even at a concentration of 1 ng/ml. No specific psychiatric disorder was favored in children of MCPD with the highest titers. We next determined whether the enrichment of ABs in the fetal circulation can lead to clearly detectable IgG titers in the pups despite negative AB results in dams using a routine ELISA. Stepwise titration of injected human IgG resulted in this “seropositivity/seronegativity” discrepancy in the 6.6  $\mu$ g group, suggesting that pregnant women testing “negative” for NR1 ABs in clinical routine assays may not exclude fetal enrichment.

## Discussion

Human IgG NR1 ABs were detected with cell-based assays in 1% of asymptomatic controls in previous studies,<sup>11,12</sup> creating a considerable subgroup of pregnant women at risk of transferring this anti-neuronal AB to the fetus. The prevalence of low-titer NR1 ABs might even be higher, as routine cell-based assays work with clear cutoff values for detection of patients with suspected NMDAR encephalitis. To model the underlying risk in mice, we administered human recombinant NR1 ABs into pregnant animals. The offspring had reduced densities of synaptic NMDAR, increased mortality, altered physiological functions, and impaired neurodevelopment. Most importantly, mild behavioral changes

persisted into adulthood and were accompanied by significantly reduced brain volumes, indicating the potential of lifelong neuropsychiatric consequences from transient exposure to maternal NR1 ABs during pregnancy. Given the increased mortality in NR1 AB-treated offspring, surviving animals might have been more mildly affected, resulting in underestimation of the AB effect.

In a translational approach, data from the present study indicate that healthy MCPD may have higher serum NR1 IgG reactivity compared to CTLM. The effect was only subtle, potentially weakened due to spontaneous fading of NR1 AB titers over time (as known from autoimmune encephalitis) given the long interval (4–20 years) between pregnancy and AB testing. We compared the continuous spectrum of NR1 autoreactivity rather than categorizing only extremely high titers (“seropositive,” which may indicate NMDAR encephalitis) as MCPD were asymptomatic (see Fig 5A). Interestingly, even below-threshold maternal serum titers of NR1 ABs may result in fetal IgG enrichment (see Fig 5C). Similar to human placental FcRn, IgG is actively transported into the fetal murine circulation via the FcRn in the yolk sac.<sup>36</sup> In contrast to humans, maternal IgG reaches the neonatal circulation in mice also via secretion into breast milk.<sup>37</sup> In both species, the fetal BBB is not fully developed,<sup>38</sup> allowing interference of ABs with fetal development while not crossing the intact maternal BBB. Binding to NMDAR might further retain and increase the ABs in the fetal brain, as in an injection model using animals with disrupted BBB.<sup>39</sup> Thus, high levels of ABs might not be required to distinguish MCPD from CTLM. In asymptomatic human mothers with low or even subthreshold

**FIGURE 2: Quantification of synaptic N-methyl-D-aspartate receptor density and characterization of electrophysiological properties in antibody (AB)-treated neonates. (A–C) Representative Western blots (cropped) of synaptosomal (A), membrane (B), and total-cell fractions (C) prepared from neonatal brains at postnatal day (P) 0 showed NR1 protein reduction, as compared with the respective reference protein. Quantification showed significant NR1 protein reduction in all 3 fractions ( $n = 8$  from 3–5 different litters; mean  $\pm$  standard deviation [SD], unpaired  $t$  test,  $p = 0.0063$  [A],  $p = 0.0365$  [B],  $p = 0.0005$  [C]). (D) Control (CTL) blots showed no reduction of  $\alpha$ -amino-3-hydroxy-5-methyl-4-isoxazolepropionic acid receptor (GluR1) protein at P0 in the total-cell fraction. (E, F, H, I) NR1 protein reduction was also observed when comparing immunohistochemistry of NR1-positive clusters (E, H) with expression of the synaptic protein Homer-1 (F, I). (G, J) The overlays demonstrated much less colocalization in NR1 AB-treated animals (J) compared to controls (G). (K) Quantification of the percentage of NR1<sup>+</sup> clusters of all Homer-1<sup>+</sup> clusters showed strong reduction at P0 ( $n = 5$  from 5 different litters, mean  $\pm$  SD, unpaired  $t$  test,  $p < 0.0001$ ), which was less pronounced at P7 ( $n = 5$  from 4–5 different litters, mean  $\pm$  SD, unpaired  $t$  test,  $p = 0.0102$ ). For cluster quantification in E–K, AB treatment was done with a monoclonal human NR1 AB (#003-102) different from the human detection AB (#007-168). This was possible as both ABs did not compete for the identical epitope (L–P), exemplarily shown for #003-102 alone (L, signal intensity measured in the hippocampal stratum radiatum [mean of the white circles] minus background fluorescence [turquoise circle]), #003-102 competing with 100  $\mu$ g/ml #003-102 (M) or 100  $\mu$ g/ml #007-168 (N, insert shows hippocampal binding of the Homer-1 AB). (P) Quantification of the respective dose curves showed that each monoclonal NR1 AB was only displaced by itself but not by the other NR1 or a Homer-1 AB ( $n = 4$  independent experiments). (Q, R) Representative recordings of spontaneous excitatory postsynaptic currents (sEPSCs) in neonatal brain slices at P0 (Q) and P7 (R). (S) Quantification revealed marked reduction of sEPSC amplitudes at P0 ( $n = 16$  [CTL] and  $n = 12$  [NR1] cells from 5 neonates from 5 different litters, mean  $\pm$  SD, unpaired  $t$  test,  $p = 0.0176$ ), which normalized until P7 ( $n = 15$  [CTL] and  $n = 12$  [NR1] cells from 6 neonates from 6 different litters,  $p = 0.088$ ). (T) sEPSC frequencies were not affected (mean  $\pm$  SD, unpaired  $t$  test,  $p = 0.0688$  [P0],  $p = 0.994$  [P7]). \* $p < 0.05$ ; \*\* $p < 0.01$ ; \*\*\* $p < 0.001$ ; \*\*\*\* $p < 0.0001$ . hum = human; n.s. = not significant.**



serum NR1 AB titers, fetal NR1 IgG might still accumulate to a degree sufficient for permanent damage to the developing brain. Also, other factors could facilitate maternofetal AB transfer and induce neuropsychiatric disease, such as inflammation, genetic risk loci, placental microstructure, or psychosocial stress ("second hits").

Support for our model also comes from previous murine models of maternal anti-neuronal ABs affecting fetal development with long-term defects in the offspring.<sup>6-9</sup> Gestational transfer of IgG from mothers of children with ASD into mice resulted in reduced sociability and increased anxiety.<sup>7,8</sup> Active immunization against the NMDAR-NR2A/-

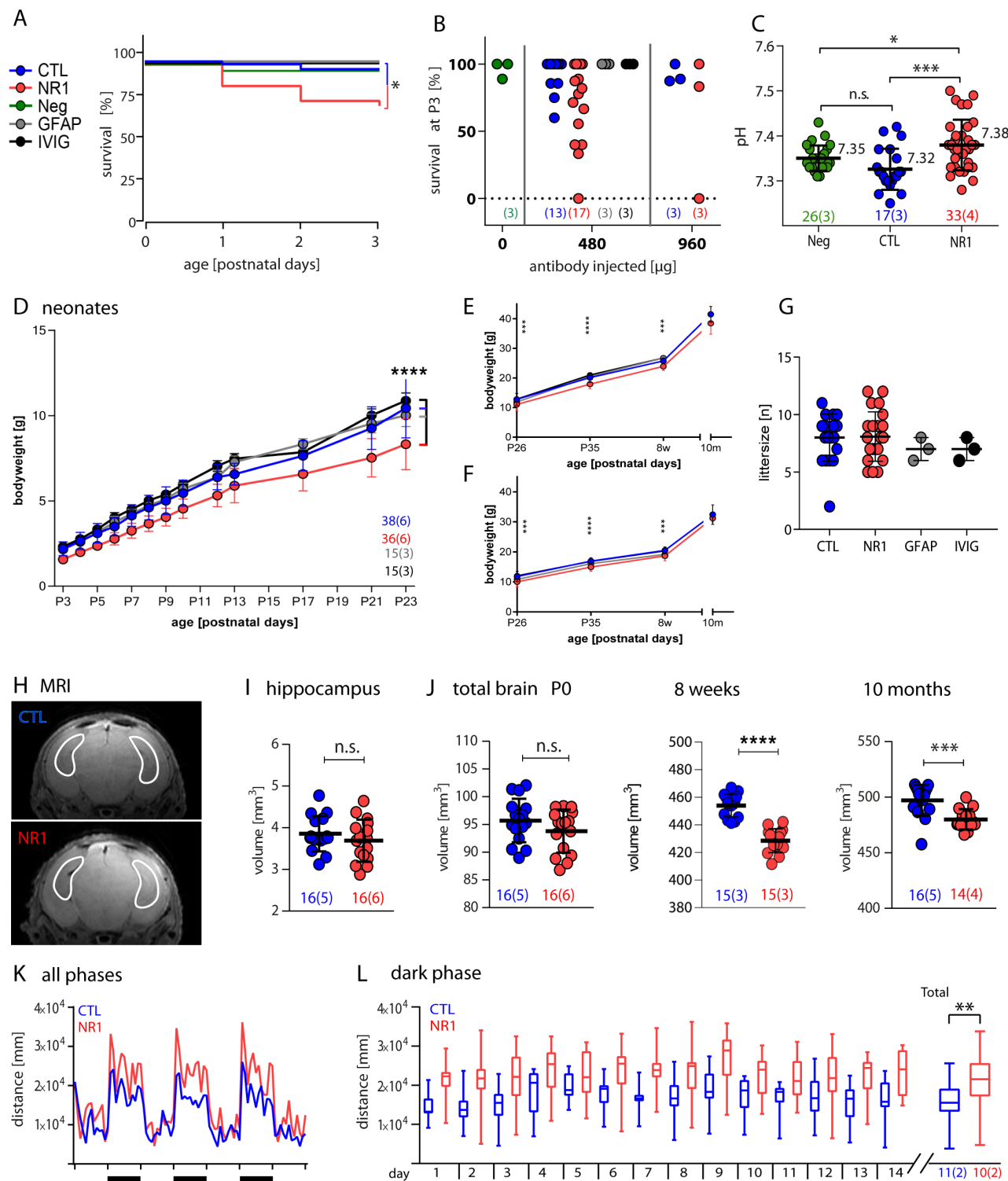


FIGURE 3: Legend on next page.

**TABLE 1. Comparison of Absolute Volumes of Different Brain Regions after 8 Weeks and 10 Months**

Region	8 Weeks		<i>p</i>	Sign.	10 Months		<i>p</i>	Sign.
	CTL, n = 15, Mean ± SD	NR1, n = 15, Mean ± SD			CTL, n = 16, Mean ± SD	NR1, n = 14, Mean ± SD		
Cerebellum	45.32 ± 0.87	40.97 ± 1.72	1.79E-9	<sup>a</sup>	48.61 ± 1.49	44.61 ± 1.23	1.23E-8	<sup>a</sup>
Midbrain	22.74 ± 0.58	21.48 ± 0.65	5.90E-6	<sup>a</sup>	24.25 ± 0.96	22.92 ± 0.50	7.00E-5	<sup>a</sup>
Brainstem	86.39 ± 1.83	80.73 ± 2.73	3.00E-7	<sup>a</sup>	93.05 ± 3.11	88.47 ± 2.32	0.0001	<sup>a</sup>
Pallidum	8.02 ± 0.31	7.50 ± 0.36	0.0002	<sup>b</sup>	9.27 ± 0.42	8.94 ± 0.22	0.0133	
Hypothalamus	12.01 ± 0.71	11.20 ± 0.47	0.0004	<sup>b</sup>	13.53 ± 0.85	12.90 ± 0.60	0.0299	
Cerebral cortex	173.83 ± 3.61	166.45 ± 2.75	8.31E-7	<sup>a</sup>	190.90 ± 5.36	187.26 ± 3.68	0.0414	
Striatum	39.99 ± 1.29	34.54 ± 1.21	1.03E-5	<sup>a</sup>	41.52 ± 1.42	40.69 ± 0.96	0.0738	
Hippocampus	35.59 ± 0.98	33.64 ± 1.06	1.52E-5	<sup>a</sup>	39.26 ± 1.56	38.58 ± 1.83	0.2780	
Thalamus	19.44 ± 0.51	18.40 ± 0.53	5.49E-6	<sup>a</sup>	21.71 ± 0.71	21.38 ± 1.02	0.3027	
Amygdala	0.96 ± 0.05	0.92 ± 0.03	0.0041	<sup>c</sup>	1.07 ± 0.05	1.06 ± 0.03	0.6579	

Probability values were not adjusted. Values are expressed in mm<sup>3</sup>. Changes in total brain volumes were treatment-specific (8 weeks: *p* < 0.0001; 10 months: *p* = 0.0015), but not sex-specific (8 weeks: *p* = 0.284; 10 months: *p* = 0.677; 2-way analysis of variance of treatment versus sex interaction).

<sup>a</sup>*p* < 0.0001; <sup>b</sup>*p* < 0.001; <sup>c</sup>*p* < 0.01.

CTL = control; SD = standard deviation; Sign. = significance level.

NR2B (GluN2A/2B) subunits in pregnant dams led to death of female fetuses, altered histological properties, and long-lasting cognitive defects in male offspring.<sup>6</sup> In another study, human recombinant Caspr2 ABs were passively transferred into mice, resulting in abnormal cortical development in male offspring with decreased dendritic complexity and

abnormal behavior.<sup>9</sup> Similarly, Caspr2 AB-containing maternal IgG fractions led to marked social interaction deficits in the offspring, disturbances in layer formation in somatosensory cortex, and increased microglial activation.<sup>10</sup>

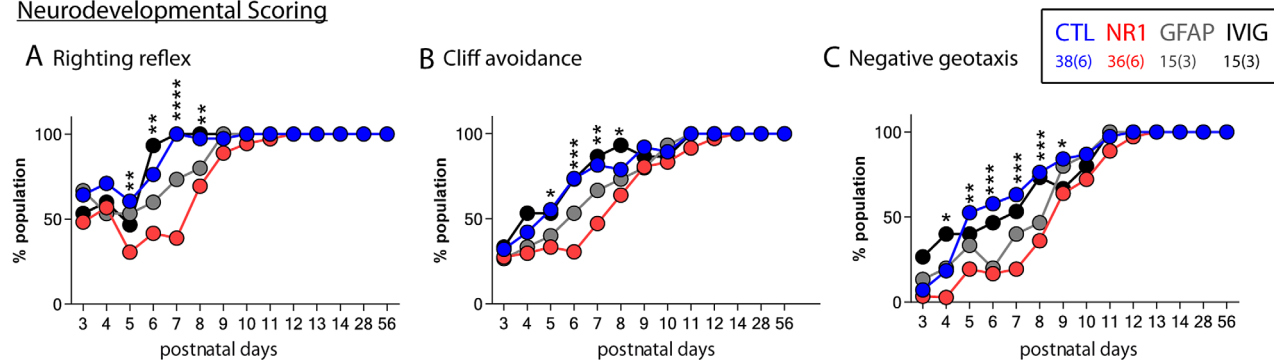
Synaptic NMDAR activity is involved in different stages of fetal and neonatal brain development, crucial for

**FIGURE 3: Mortality and physiological parameters of control (CTL) and NR1 antibody (AB)-treated offspring. (A)** Kaplan–Meier analysis of neonate survival showed significantly increased mortality in NR1 AB-treated animals (log-rank test, corrected with Bonferroni correction for *K* = 5, adjusted *p* = 0.025 [NR1 vs CTL]) compared to all 4 control groups. **(B)** Survival rates of untreated, CTL, glial fibrillary acidic protein (GFAP), intravenous immunoglobulin (IVIG), and NR1 AB-treated neonates at postnatal day (P) 3 with different doses (untreated: *n* = 3 litters; 480μg: *n* = 13 [CTL], *n* = 17 [NR1], *n* = 3 [GFAP], *n* = 3 [IVIG]; 960μg: *n* = 3 [CTL], *n* = 3 [NR1]). **(C)** Blood pH of untreated, CTL, and NR1 AB-treated neonates at P0 showed significantly elevated pH in the NR1 group (untreated: *n* = 26 from 3 litters; CTL ABs: *n* = 17 from 3 litters; NR1 ABs: *n* = 33 from 4 litters; mean ± standard deviation [SD], 1-way analysis of variance [ANOVA], post hoc Tukey multiple comparison test, untreated vs CTL ABs: *p* = 0.1685; untreated vs NR1 ABs: *p* = 0.0488; CTL vs NR1 ABs: *p* = 0.0002). **(D–F)** Development of body weight of breastfed neonates (D), females (E), and males (F) after weaning (mean ± SD, repeated measures ANOVA, Sidak multiple comparison test, *p* < 0.0001 for NR1 vs all 3 control groups). **(G)** Litter size did not differ between all treatment groups (*n* = 17 [CTL], *n* = 20 [NR1], *n* = 3 [GFAP], *n* = 3 [IVIG]). **(H)** Representative brain magnetic resonance imaging (MRI) of CTL and NR1 AB-treated neonates (hippocampal regions highlighted). **(I, J)** MRI-based quantification showed similar volumes at P0 in both groups for hippocampus (I; *n* = 16, mean ± SD, unpaired *t* test, *p* = 0.3158) and total brain (J [left]; *n* = 16, mean ± SD, unpaired *t* test, *p* = 0.176). With long follow-up, total brain volumes of 8-week-old (J [middle]; CTL, *n* = 15; NR1, *n* = 15; mean ± SD, unpaired *t* test, *p* = 0.0001) and 10-month-old mice (J [right]; CTL, *n* = 16; NR1, *n* = 14; mean ± SD, unpaired *t* test, *p* = 0.0005) showed highly significant differences in total brain volumes. **(K)** Typical activity (mean of distance traveled) in home cages during 3 dark (*black bars*) and 4 light phases of adult offspring. **(L)** In dark phases, home cage activity (boxplots of distance traveled) of NR1 (*n* = 10) compared to CTL AB-treated animals (*n* = 11) was consistently higher during 14 days and in total (boxplots: median, 25th–75th quartile, minimum–maximum; Wilcoxon test of dark phase over all days, test score = 179, *p* = 0.0049). \**p* < 0.05; \*\**p* < 0.01; \*\*\**p* < 0.001; \*\*\*\**p* < 0.0001. n.s. = not significant.

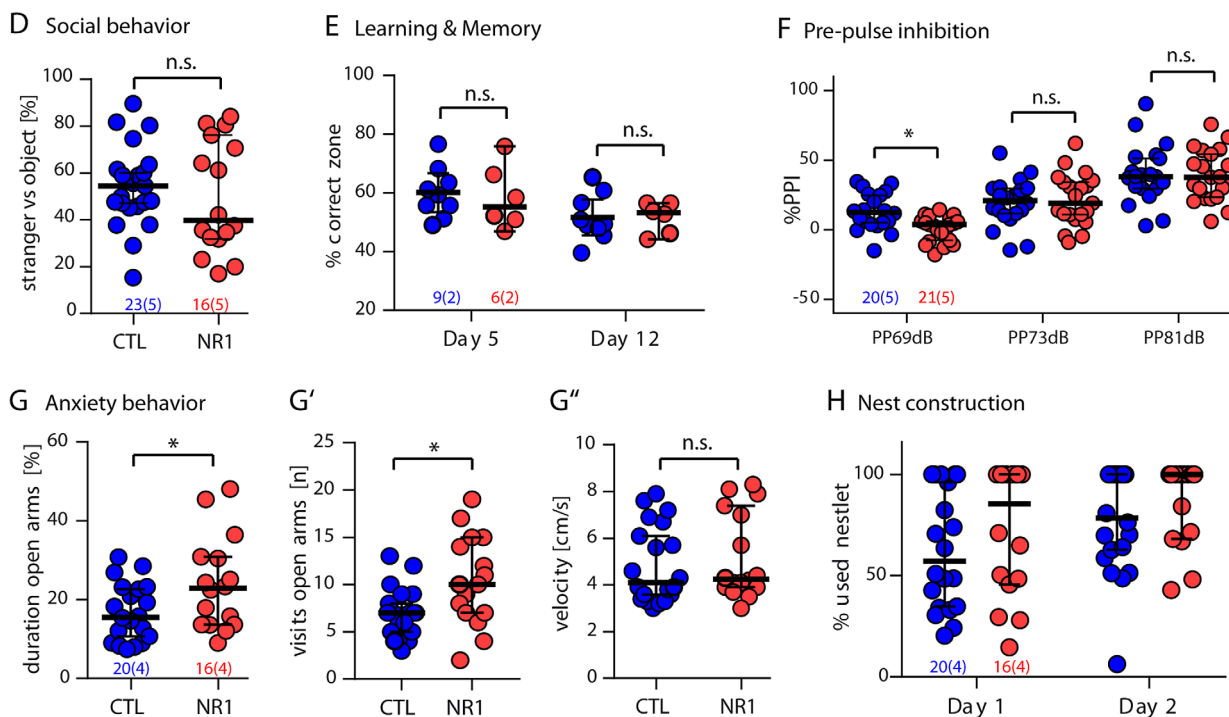
circuit development and map formation, and deletion of the NR1 subunit is lethal.<sup>40</sup> In accordance with other in vitro and in vivo studies,<sup>14,15</sup> we here showed removal

of NMDAR from the surface. This reduction was accompanied by decreased amplitudes of AMPAR-mediated sEPSCs, only present in young neonates (P0). Despite the

Neurodevelopmental Scoring



Behavioral tasks



Natural behavior

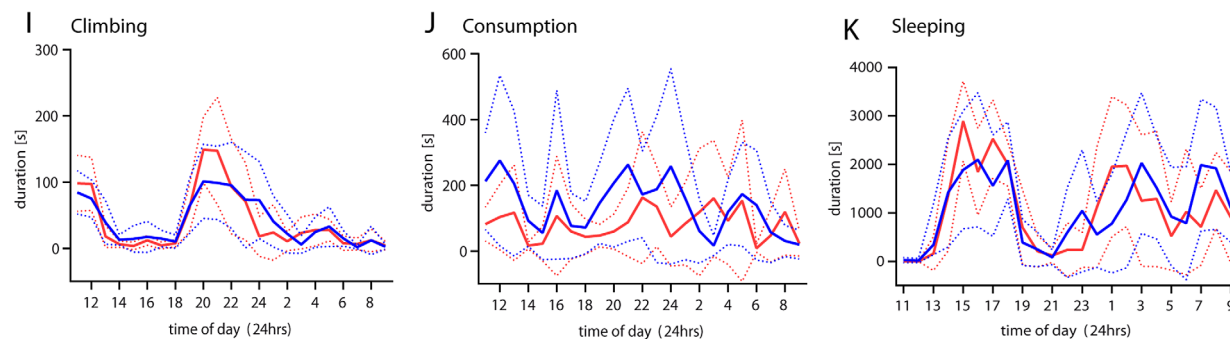
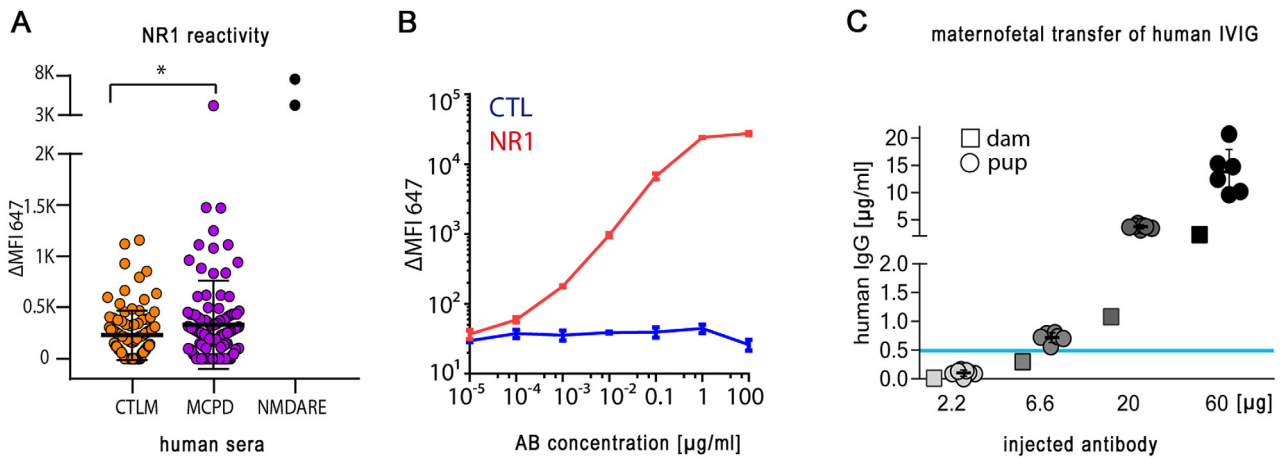


FIGURE 4: Legend on next page.



**FIGURE 5:** Serum NR1 autoreactivity in mothers of children with psychiatric disorders (MCPD) compared to healthy control mothers of unaffected children (CTLM). (A) Antibody (AB) reactivity (median fluorescence intensity [ $\Delta$ MFI]) of sera against NR1-expressing HEK cells was increased in MCPD ( $n = 120$ ) versus CTLM ( $n = 105$ , mean  $\pm$  SD; unpaired  $t$  test,  $*p = 0.038$ ). Serum of *N*-methyl-D-aspartate receptor encephalitis (NMDARE) patients served as positive controls (right;  $n = 2$ ). (B) The flow cytometry assay showed high sensitivity even in the low ng/ml range as validated with monoclonal human NR1 versus control (CTL) ABs. (C) Increasing doses of maternally injected human immunoglobulins consistently resulted in murine fetal AB enrichment. A given AB dose (here single maternal injection of 6.6  $\mu$ g human IgG) can lead to clearly detectable titers in pups (circles), whereas it remains under the detection threshold (blue line,  $<0.5 \mu$ g/ml in this routine enzyme-linked immunosorbent assay) in the mother (rectangles). IVIG = intravenous immunoglobulin.

lack of data for direct NMDAR function, affected AMPAR-mediated signaling was treatment-specific, and likely resulted from disrupted NMDAR-mediated insertion of AMPAR,<sup>20</sup> normalizing at P7. The seeming discrepancy between increasing postpartum AB levels in serum and brain versus decreasing effects on NMDAR density and function indicate an early developmental window of high susceptibility. At this time, NMDAR are primarily responsible for glutamatergic transmission but are expressed at low levels. Thus, they cannot compensate the NR1 AB-mediated detrimental effect, whereas this is likely possible when NMDAR expression increases considerably later on.

Defects in our NR1 AB-treated animals likely were related to NMDAR dysfunction, as they resembled genetic and autoimmune models. For example, affected neonates had  $>27\%$  increased mortality in the first postnatal days and markedly increased blood pH, a clinical parameter of acid-base metabolism and respiratory function. Loss-of-function mutations in the NR1 gene were lethal,<sup>22</sup> and NR1 knockout mice died within 8 to 15 hours after birth due to respiratory failure.<sup>41</sup> Small neonatal blood volumes prevented additional measurement of  $p\text{CO}_2$ ,  $p\text{O}_2$ , or  $\text{HCO}_3$  levels from further determining respiratory, neuromuscular, and metabolic contributions. Genetic models usually showed a more

**FIGURE 4:** Neurodevelopmental and behavioral impairment from postnatal to adult mice in NR1 antibody (AB)-treated offspring. (A–C) Delayed development of the righting reflex (A), cliff avoidance (B), and negative geotaxis (C) in NR1 AB-treated neonates compared to controls (3–6 litters,  $n = 17$  [control (CTL)],  $n = 14$  [NR1],  $n = 15$  [glial fibrillary acidic protein (GFAP)],  $n = 15$  [intravenous immunoglobulin (IVIG)]), points symbolize % of population showing the respective reflex, 1-sided Fisher exact test for each day;  $*p < 0.05$ ;  $**p < 0.01$ ;  $***p < 0.001$ ;  $****p < 0.0001$ , NR1 vs CTL). (D) Normal social preference of adolescent mice from both treatment groups ( $n = 23$  [CTL],  $n = 16$  [NR1] from 5 litters, median  $\pm$  95% confidence interval [CI], Mann–Whitney  $U$  test,  $p = 0.4115$ ). (E) Memory recall in the Barnes maze was not impaired 1 and 7 days after learning ( $n = 9$  [CTL],  $n = 6$  [NR1] from 2 litters, median  $\pm$  95% CI, Kruskal–Wallis-test,  $p = 0.1322$ ). (F) Prepulse inhibition (PPI) determined by startle reaction showed impaired sensorimotor gating in NR1 AB-treated mice ( $n = 20$  [CTL],  $n = 21$  [NR1] from 5 litters, median  $\pm$  95% CI, Kruskal–Wallis test with Dunn post hoc test: PP69dB,  $p = 0.0263$ ; PP73dB,  $p = 0.7964$ ; PP81dB,  $p = 0.9650$ ). (G, G') Anxiety was lower in the NR1 group as displayed by longer duration in open arms (G,  $n = 20$  [CTL],  $n = 16$  [NR1] from 4 litters, median  $\pm$  95% CI, Mann–Whitney  $U$  test,  $p = 0.0494$ ) and increased number of entries into open arms of the elevated plus maze (G',  $p = 0.0139$ ). (G'') Velocity was not affected by AB treatment ( $p = 0.3475$ ). (H) Nest construction was normal as measured by the weight of unused nest material ( $n = 20$  [CTL],  $n = 16$  [NR1] from 4 litters, median  $\pm$  95% CI, Kruskal–Wallis test,  $p = 0.0718$ ). (I–K) Individual behavior was recorded with a HomeCageScan system for each mouse and did not show significant differences in any recorded behavior, including climbing behavior (I; CTL,  $n = 9$ ; NR1,  $n = 6$ , mean  $\pm$  SD [dotted lines], repeated measures analysis of variance; between-subject factor  $p = 0.9957$ ), consumption (eating + drinking) behavior (J; between-subject factor  $p = 0.1857$ ), and sleeping behavior (K;  $p = 0.9628$ ). n.s. = not significant; N = white noise; P = pulse; PP = prepulse.

**TABLE 2. Cohort Characteristics of Matched Mothers of Children with Psychiatric Disorders (n = 120, Mean Age = 42.3 ± 7.8 Years) and Healthy Control Mothers of Unaffected Children (n = 105, Mean Age = 43.6 ± 9.7 Years)**

ICD-10	Disorder Classification	Cases	Disorder	
			M	F
F1	Mental and behavioral disorders due to psychoactive substance use	2	1	1
F2	Schizophrenia, schizotypal, and delusional disorders	2	1	1
F3	Mood (affective) disorders	22	6	16
F4	Neurotic, stress-related, and somatoform disorders	19	11	8
F5	Behavioral syndromes associated with physiological disturbances and physical factors	1	0	1
F6	Disorders of adult personality and behavior	2	0	2
F7	Mental retardation	1	1	0
F84	Pervasive developmental disorders	8	8	0
F90	Attention-deficit hyperactivity disorders	32	24	8
F91; F92	Conduct disorders; mixed disorders of conduct and emotions	20	11	9
F93; F94; F98	Emotional disorders with onset specific to childhood; disorders of social functioning with onset specific to childhood and adolescence; other behavioral and emotional disorders with onset usually occurring in childhood and adolescence	12	9	3

Diagnoses of psychiatric disorders were coded according to the German modification of the ICD-10 as provided within health insurance data.

F = female; ICD-10 = International Classification of Diseases and Related Health Problems, 10th Revision; M = male.

severe phenotype, whereas NR1 AB-treated animals performed well in paradigms of social behavior, spatial learning, and nest construction, which is likely related to normalization of NMDAR function with fading AB titers. Clinical experience with pregnant NMDAR encephalitis patients further supports the pathogenic effects of in utero exposure to human NR1 ABs<sup>42–46</sup> and even demonstrated 4-fold higher titers in a newborn.<sup>45</sup> Obvious neonatal developmental impairment was seen in approximately half of the babies.<sup>47</sup> The lack of follow-ups prevented any conclusion on potential further deficits with later onset. Midgestational sera from a Danish biobank revealed significantly higher frequencies of NMDAR ABs (29%) in mothers with schizophrenia spectrum disorders (SSD) whose children were diagnosed with mental retardation and disorders of psychological development, compared to mothers with SSD and unaffected children.<sup>48</sup> Such difference was not seen in mothers without SSD.<sup>48</sup>

Offspring from our murine study displayed behavioral signs resembling several models of neuropsychiatric developmental disorders. For example, surviving animals showed impaired neurodevelopment, lower bodyweight, and delayed neonatal sensory–motor reflexes, similar to gestational transfer models of ASD<sup>7</sup> and learning disabilities related to anti-NR2A/B ABs.<sup>6</sup> In humans, motor delays are observed in 51% of individuals with ASD.<sup>49</sup> Moreover, behavioral changes manifesting later in life in NR1 AB-treated animals included elevated activity, decreased anxiety behavior in the elevated plus maze, and partially reduced PPI. Hyperlocomotion is a hallmark of several neuropsychiatric disorders, such as attention-deficit/hyperactivity disorder (ADHD), bipolar disorders, and schizophrenia, in both humans and rodent models<sup>50</sup> and in mice with reduced NMDAR expression.<sup>51,52</sup> Reduction of anxiety was equally well documented in ADHD models.<sup>53</sup> Finally, NR1 AB-treated animals were similar to animals with reduced NMDAR expression by decreased PPI, reflecting impaired sensorimotor gating and preconscious attention.<sup>50–52</sup> PPI is reduced not only in schizophrenia, but also in psychotic bipolar disorder and ADHD.<sup>54</sup>

The findings collectively suggest that diaplacentally transferred NR1 ABs are not linked to a single (NMDAR encephalitis-like) disorder, but could potentially contribute to a broader spectrum of behavioral abnormalities found in ADHD, ASD, bipolar disorders, schizophrenia, or learning disabilities. In line with this hypothesis, maternal NR1 ABs induced long-lasting neuropathological effects in the offspring, with reduced volumes of several brain areas in old mice. The mechanisms behind the delayed development of pathological changes require further

research and may include dysfunctional formation of cortical layers or NR1-mediated effects on progenitor cells.<sup>55</sup> Thus, gestational NR1 AB exposure may primarily be seen as a neurodevelopmental congenital brain disorder that is potentially amenable to immunotherapy, thus clearly deserving detailed analyses in future animal and prospective human studies with long follow-up. These should determine the kinetics of AB titers over time in mothers and neonates, presence of clinical neuropsychiatric symptoms and developmental delays, and contribution of additional risk factors.

## Acknowledgment

This study was supported by grants from the German Research Foundation (DFG; to H.P.: PR1274/2-1; to S. Mu., P.B.-S., and U.D.: Excellence Cluster NeuroCure) and from the Federal Ministry of Education and Research (to S. Mu., P.B.-S., and U.D.: 01EO0801, Center for Stroke Research Berlin). S.Ma. was supported by postdoctoral fellowships from the European Molecular Biology Organization (ALTF\_393-2015) and the DFG (MA 7374/1-1).

We thank D. Brandl for excellent technical help, T. Frey for characterization of ATD-Fc construct used for anti-NR1 ELISA, S. Amrei-Kunde for help with planning and analyzing Western blot experiments, Dr S. P. Koch for analysis of MRI scans of adult mice.

This work is part of B.J.'s PhD thesis. Datasets are publicly available and can be accessed at <https://figshare.com/s/bfb41d12865ca5efc4e5>.

## Author Contributions

B.J., M.C., J.K., K.L., U.D., D.S., M.K., and H.P. contributed to the conception and design of the study; B.J., M.C., J.K., K.L., L.K., P.F., H.-C.K., L.-M.D., N.K.W., M.L., M.R., Y.W., J.L., J.H., S.Ma., S.Mu., P.B.-S., M.K., and H.P. contributed to the acquisition and analysis of data; B.J., M.C., J.K., L.K., H.-C.K., L.-M.D., D.S., M.K., and H.P. contributed to drafting the text and preparing the figures.

## Potential Conflicts of Interest

Nothing to report.

## References

- Kowal C, Athanassiou A, Chen H, Diamond B. Maternal antibodies and developing blood-brain barrier. *Immunol Res* 2015;63:18–25.
- Palmeira P, Quinello C, Silveira-Lessa AL, et al. IgG placental transfer in healthy and pathological pregnancies. *Clin Dev Immunol* 2012; 2012:985646.
- Kumar MA, Jain A, Dechant VE, et al. Anti-N-methyl-D-aspartate receptor encephalitis during pregnancy. *Arch Neurol* 2010;67:884–887.
- Estes ML, McAllister AK. Maternal immune activation: implications for neuropsychiatric disorders. *Science* 2016;353:772–777.
- Fox E, Amaral D, Van de Water J. Maternal and fetal antibrain antibodies in development and disease. *Dev Neurobiol* 2012;72: 1327–1334.
- Lee JY, Huerta PT, Zhang J, et al. Neurotoxic autoantibodies mediate congenital cortical impairment of offspring in maternal lupus. *Nat Med* 2009;15:91–96.
- Braunschweig D, Golub MS, Koenig CM, et al. Maternal autism-associated IgG antibodies delay development and produce anxiety in a mouse gestational transfer model. *J Neuroimmunol* 2012;252:56–65.
- Singer HS, Morris C, Gause C, et al. Prenatal exposure to antibodies from mothers of children with autism produces neurobehavioral alterations: a pregnant dam mouse model. *J Neuroimmunol* 2009;211: 39–48.
- Brimberg L, Mader S, Jeganathan V, et al. Caspr2-reactive antibody cloned from a mother of an ASD child mediates an ASD-like phenotype in mice. *Mol Psychiatry* 2016;21:1663–1671.
- Coutinho E, Menassa DA, Jacobson L, et al. Persistent microglial activation and synaptic loss with behavioral abnormalities in mouse offspring exposed to CASPR2-antibodies in utero. *Acta Neuropathol* 2017;134:567–583.
- Dahm L, Ott C, Steiner J, et al. Seroprevalence of autoantibodies against brain antigens in health and disease. *Ann Neurol* 2014;76: 82–94.
- Lang K, Prüss H. Frequencies of neuronal autoantibodies in healthy controls: estimation of disease specificity. *Neurol Neuroimmunol Neuroinflamm* 2017;4:e386.
- Kreye J, Wenke NK, Chayka M, et al. Human cerebrospinal fluid monoclonal N-methyl-D-aspartate receptor autoantibodies are sufficient for encephalitis pathogenesis. *Brain* 2016;139:2641–2652.
- Hughes EG, Peng X, Gleichman AJ, et al. Cellular and synaptic mechanisms of anti-NMDA receptor encephalitis. *J Neurosci* 2010; 30:5866–5875.
- Planaguma J, Leypoldt F, Mannara F, et al. Human N-methyl D-aspartate receptor antibodies alter memory and behaviour in mice. *Brain* 2015;138:94–109.
- Malviya M, Barman S, Golombeck KS, et al. NMDAR encephalitis: passive transfer from man to mouse by a recombinant antibody. *Ann Clin Transl Neurol* 2017;4:768–783.
- Cline HT, Debski EA, Constantine-Paton M. N-methyl-D-aspartate receptor antagonist desegregates eye-specific stripes. *Proc Natl Acad Sci U S A* 1987;84:4342–4345.
- Wu GY, Zou DJ, Rajan I, Cline H. Dendritic dynamics in vivo change during neuronal maturation. *J Neurosci* 1999;19:4472–4483.
- Hardingham GE, Bading H. Synaptic versus extrasynaptic NMDA receptor signalling: implications for neurodegenerative disorders. *Nat Rev Neurosci* 2010;11:682–696.
- Leinekugel X, Medina I, Khalilov I, et al. Ca<sup>2+</sup> oscillations mediated by the synergistic excitatory actions of GABA(A) and NMDA receptors in the neonatal hippocampus. *Neuron* 1997;18:243–255.
- Stefani MR, Moghaddam B. Transient N-methyl-D-aspartate receptor blockade in early development causes lasting cognitive deficits relevant to schizophrenia. *Biol Psychiatry* 2005;57:433–436.
- Single FN, Rozov A, Burnashev N, et al. Dysfunctions in mice by NMDA receptor point mutations NR1(N598Q) and NR1(N598R). *J Neurosci* 2000;20:2558–2566.
- Ly LT, Kreye J, Jurek B, et al. Affinities of human NMDA receptor autoantibodies: implications for disease mechanisms and clinical diagnostics. *J Neurol* 2018;265:2625–2632.
- Wenke NK, Kreye J, Andrzejak E, et al. N-methyl-D-aspartate receptor dysfunction by unmutated human antibodies against the NR1 subunit. *Ann Neurol* 2019;85:771–776.

25. Dalton P, Deacon R, Blamire A, et al. Maternal neuronal antibodies associated with autism and a language disorder. *Ann Neurol* 2003; 53:533–537.
26. Dawes JM, Weir GA, Middleton SJ, et al. Immune or genetic-mediated disruption of CASPR2 causes pain hypersensitivity due to enhanced primary afferent excitability. *Neuron* 2018;97: 806–822.e10.
27. Wardemann H, Yurasov S, Schaefer A, et al. Predominant autoantibody production by early human B cell precursors. *Science* 2003; 301:1374–1377.
28. Garty BZ, Ludomirsky A, Danon YL, et al. Placental transfer of immunoglobulin G subclasses. *Clin Diagn Lab Immunol* 1994;1:667–669.
29. Paoletti LC, Pinel J, Kennedy RC, Kasper DL. Maternal antibody transfer in baboons and mice vaccinated with a group B streptococcal polysaccharide conjugate. *J Infect Dis* 2000;181:653–658.
30. Koch S, Mueller S, Foddiss M, et al. Atlas registration for edema-corrected MRI lesion volume in mouse stroke models. *J Cereb Blood Flow Metab* 2019;39:313–323.
31. Heyser CJ. Assessment of developmental milestones in rodents. *Curr Protoc Neurosci* 2004;Chapter 8:Unit 8.18.
32. Rogers DC, Peters J, Martin JE, et al. SHIRPA, a protocol for behavioral assessment: validation for longitudinal study of neurological dysfunction in mice. *Neurosci Lett* 2001;306:89–92.
33. Lipina T, Labrie V, Weiner I, Roder J. Modulators of the glycine site on NMDA receptors, D-serine and ALX 5407, display similar beneficial effects to clozapine in mouse models of schizophrenia. *Psychopharmacology (Berl)* 2005;179:54–67.
34. Deacon R. Assessing burrowing, nest construction, and hoarding in mice. *J Vis Exp* 2012;(59):e2607.
35. Chourbaji S, Hoyer C, Richter SH, et al. Differences in mouse maternal care behavior—is there a genetic impact of the glucocorticoid receptor? *PLoS One* 2011;6:e19218.
36. Kim J, Mohanty S, Ganesan LP, et al. FcRn in the yolk sac endoderm of mouse is required for IgG transport to fetus. *J Immunol* 2009;182: 2583–2589.
37. Van de Perre P. Transfer of antibody via mother's milk. *Vaccine* 2003;21:3374–3376.
38. Braniste V, Al-Asmakh M, Kowal C, et al. The gut microbiota influences blood-brain barrier permeability in mice. *Sci Transl Med* 2014; 6:263ra158.
39. Castillo-Gomez E, Kastner A, Steiner J, et al. The brain as immunoprecipitator of serum autoantibodies against N-Methyl-D-aspartate receptor subunit NR1. *Ann Neurol* 2016;79:144–151.
40. Ewald RC, Cline HT. NMDA receptors and brain development. In: Van Dongen AM, ed. *Biology of the NMDA receptor*. Boca Raton, FL: Taylor & Francis, 2009:1–18.
41. Forrest D, Yuzaki M, Soares HD, et al. Targeted disruption of NMDA receptor 1 gene abolishes NMDA response and results in neonatal death. *Neuron* 1994;13:325–338.
42. Hilderink M, Titulaer MJ, Schreurs MW, et al. Transient anti-NMDAR encephalitis in a newborn infant due to transplacental transmission. *Neurol Neuroimmunol Neuroinflamm* 2015;2:e126.
43. Jagota P, Vincent A, Bhidayasiri R. Transplacental transfer of NMDA receptor antibodies in an infant with cortical dysplasia. *Neurology* 2014;82:1662–1663.
44. Mathis S, Pin JC, Pierre F, et al. Anti-NMDA receptor encephalitis during pregnancy: a case report. *Medicine (Baltimore)* 2015;94: e1034.
45. Chourasia N, Watkins MW, Lankford JE, et al. An infant born to a mother with anti-N-Methyl-d-aspartate receptor encephalitis. *Pediatr Neurol* 2018;79:65–68.
46. Ueda A, Nagao R, Maeda T, et al. Absence of serum anti-NMDAR antibodies in anti-NMDAR encephalitis mother predicts having healthy newborn. *Clin Neurol Neurosurg* 2017;161:14–16.
47. Shi YC, Chen XJ, Zhang HM, et al. Anti-N-methyl-d-aspartate receptor (NMDAR) encephalitis during pregnancy: clinical analysis of reported cases. *Taiwan J Obstet Gynecol* 2017;56:315–319.
48. Coutinho E, Jacobson L, Pedersen MG, et al. CASPR2 autoantibodies are raised during pregnancy in mothers of children with mental retardation and disorders of psychological development but not autism. *J Neurol Neurosurg Psychiatry* 2017;88:718–721.
49. Ming X, Brimacombe M, Wagner GC. Prevalence of motor impairment in autism spectrum disorders. *Brain Dev* 2007;29:565–570.
50. Powell CM, Miyakawa T. Schizophrenia-relevant behavioral testing in rodent models: a uniquely human disorder? *Biol Psychiatry* 2006;59: 1198–1207.
51. Gandal MJ, Anderson RL, Billingslea EN, et al. Mice with reduced NMDA receptor expression: more consistent with autism than schizophrenia? *Genes Brain Behav* 2012;11:740–750.
52. Mohn AR, Gainetdinov RR, Caron MG, Koller BH. Mice with reduced NMDA receptor expression display behaviors related to schizophrenia. *Cell* 1999;98:427–436.
53. Ueno KI, Togashi H, Mori K, et al. Behavioural and pharmacological relevance of stroke-prone spontaneously hypertensive rats as an animal model of a developmental disorder. *Behav Pharmacol* 2002; 13:1–13.
54. Levin R, Calzavara MB, Santos CM, et al. Spontaneously hypertensive rats (SHR) present deficits in prepulse inhibition of startle specifically reverted by clozapine. *Prog Neuropsychopharmacol Biol Psychiatry* 2011;35:1748–1752.
55. Mayer S, Chen J, Velmeshev D, et al. Multimodal single-cell analysis reveals physiological maturation in the developing human neocortex. *Neuron* 2019;102:1–16.